

Magnetoelectric Effect in the Antiferromagnetic Ordered State of Ce_3TiBi_5 with Ce Zig-Zag Chains

Masahiro Shinozaki¹, Gaku Motoyama^{1,*}, Masahiro Tsubouchi¹, Masumi Sezaki¹, Jun Gouchi², Shijo Nishigori^{1,3}, Tetsuya Mutou¹, Akira Yamaguchi⁴, Kenji Fujiwara¹, Kiyotaka Miyoshi¹, Yoshiya Uwatoko²

¹*Graduate School of Material Science, Shimane University, Matsue, Shimane 690-8504, Japan*

²*Institute for Solid State Physics, University of Tokyo, Kashiwa, Chiba 277-8581, Japan*

³*ICSR, Shimane University, Matsue, Shimane 690-8504, Japan*

⁴*Graduate School of Material Science, University of Hyogo, Ako-gun, Hyogo 678-1297, Japan*

In this study, we investigate the magnetoelectric (ME) effect of the newly discovered antiferromagnetic (AFM) compound Ce_3TiBi_5 with a hexagonal structure (space group $P6_3/mcm$). In this system, Ce ions form zig-zag chains that extend along the c -axis. We focus on the lack of the local inversion symmetry at the Ce site, although the crystal structure has an inversion center. A theoretical study has predicted that magnetization can be induced by an electric current in the AFM ordering on the zig-zag chain. We conducted magnetization measurements on Ce_3TiBi_5 under an applied constant electric current and a static magnetic field around the AFM ordering temperature of $T_N = 5.0$ K. We successfully observed of the current-induced magnetization below T_N . The magnitude of the current-induced magnetization has a linear electric current dependence and exhibits no magnetic field dependence. This behavior is consistent with the theoretical prediction of the ME effect in the ferrotoroidal ordered state.

Magnetoelectric (ME) effect has attracted considerable attention in not only some dielectric materials but also some metallic compounds. The ME effect has been discovered in chromium oxide as electric-field-induced magnetization.¹⁻³⁾ In multiferroic materials, large ME responses have been extensively studied, where electric polarization was induced by magnetic field.⁴⁻⁷⁾ On the other hand, some theoretical studies pointed out that a spontaneous toroidal order can be realized in a metallic compound by specific magnetic ordering on the

*motoyama@riko.shimane-u.ac.jp

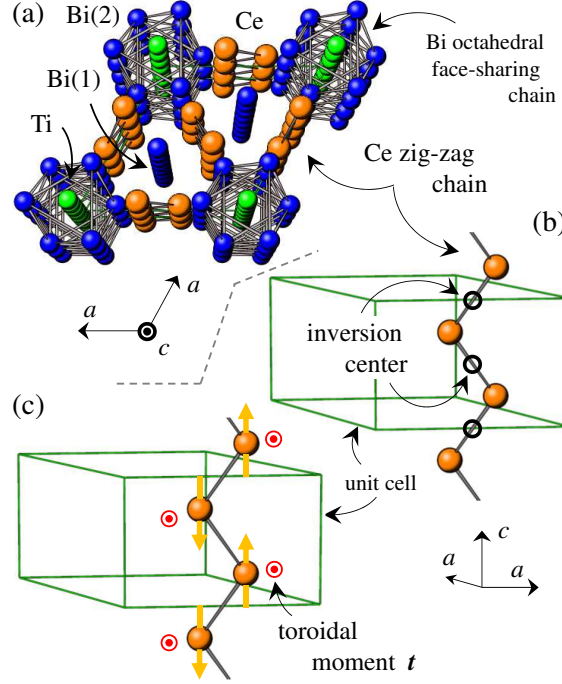


Fig. 1. (Color online) (a) Top view of the crystal structure of Ce_3TiBi_5 (space group $P6_3/mcm$). Crystallographic data: $a = 9.611$ and $c = 6.425$ Å; Ce in site $6g$ at $0.3822, 0, 3/4$; Ti in $2b$ at $0, 0, 0$; Bi(1) in $4d$ at $1/3, 2/3, 0$; and Bi(2) in $6g$ at $0.2556, 0, 1/4$. (b) Schematic side view of the crystal structure, where only Ce ions on a front side are drawn for clarity. Green line denotes a unit cell. Black circles indicate the position of the inversion center. (c) Magnetic structure on the Ce zig-zag chain, where the unit cell does not change even at the ordered state. Orange arrows on the Ce ions indicate ordered magnetic moments below T_N , which is expected from the anisotropy of $\chi(T)$.¹⁷⁾ The red mark denotes a toroidal moment on a Ce ion.

magnetic site with local inversion symmetry breaking.^{8–12)} Ferroic toroidal ordering provides various exotic cross-correlated phenomena such as the ME effect. These theoretical studies have demonstrated that spatially extended odd-parity multipoles are useful for understanding the cross-correlated phenomena. The ME effect in the ferroic toroidal ordering differs from the Edelstein effect because the Edelstein effect can occur on a crystal structure without an inversion center and is induced by a broken time reversal symmetry by applying an electric current.^{13–15)} Recently, current-induced magnetization owing to the ferroic toroidal ordering has been experimentally observed in the magnetic ordered state of UNi_4B with a layered honeycomb structure.¹⁶⁾

In this Letter, we report the discovery of the ME effect in an antiferromagnetic (AFM) phase of a new metallic compound Ce_3TiBi_5 . Ce_3TiBi_5 has a hexagonal structure with a $P6_3/mcm$ symmetry and exhibits AFM ordering at $T_N = 5.0$ K.¹⁷⁾ The crystal structure with a top view along the c -axis and a side view are shown in Figs. 1(a) and 1(b), respectively; in

the side view, only Ce atoms on the front side are shown for clarity. Figure 1(c) shows the magnetic structure on the Ce zig-zag chain. Although the details of the magnetic structure are still unknown, it is expected from the anisotropy of magnetic susceptibility below T_N that the Ce magnetic moments are almost parallel to the c -axis.¹⁷⁾ Because the crystal structure has an inversion center, Ce_3TiBi_5 does not show any current-induced magnetization in terms of the Edelstein effect. However, the inversion center exists at the midpoint of the nearest Ce-Ce bond but not at the Ce site. Ce ions form a zig-zag chain structure parallel to the c -axis. Therefore, Ce_3TiBi_5 is an attractive candidate for studying the ME effect in terms of the augmented multipole.

The AFM ordered state in this system is equivalent to the ferroic toroidal ordered state. The ordered toroidal moment vector is perpendicular to the plane containing the ordered magnetic moment vector and the position vector from the inversion center to the Ce site. It is oriented in the same direction and is denoted by the red circled dots, as shown in Fig. 1(c). Therefore, when the current is applied parallel to the a -axis, current-induced magnetization is expected to be observed on the c -axis below T_N . The sign of the induced magnetization cannot be determined until a magnetic transition occurs because there are two equivalent AFM states with oppositely oriented magnetic moments in our simple expected magnetic structure. We carried out measurements on this geometry. Specifically, magnetization in the c -axis was measured by applying a small magnetic field parallel to the c -axis and an electric current along the a -axis. We present our observation of the current-induced magnetization and discuss electric current and magnetic field dependences in Ce_3TiBi_5 .

Single crystals of Ce_3TiBi_5 were grown by the Bi self-flux method. The purities of the starting materials of Ce, Ti, and Bi were 99.9%, 99.9%, and 99.99%, respectively. These materials with a Ce:Ti:Bi ratio of 3:1:30 were placed in an alumina crucible and sealed under high vacuum conditions in a quartz tube. The sealed ampule was heated up to 1000 °C, maintained at that temperature for 11 h, and cooled slowly at 2 °C/h to 500 °C. After removing excess bismuth flux using a centrifuge, several needle-shaped crystals were obtained. The composition ratios of the obtained samples were determined using energy-dispersive X-ray spectroscopy (EDS, JEOL JSM-7001FA) and inductively coupled plasma atomic emission spectroscopy (ICP-AES, Perkin-Elmer OPTIMA 3300DV). The composition was determined as Ce:Ti:Bi = 3:1:5 within the accuracy. Sample characterizations of single-crystal specimens were carried out by X-ray diffraction (Rigaku XtaLAB). The measured Bragg reflections (2000 ~ 12000) were successfully indexed for the space group of $P6_3/mcm$.

Magnetization measurements were performed with a commercial SQUID magnetometer

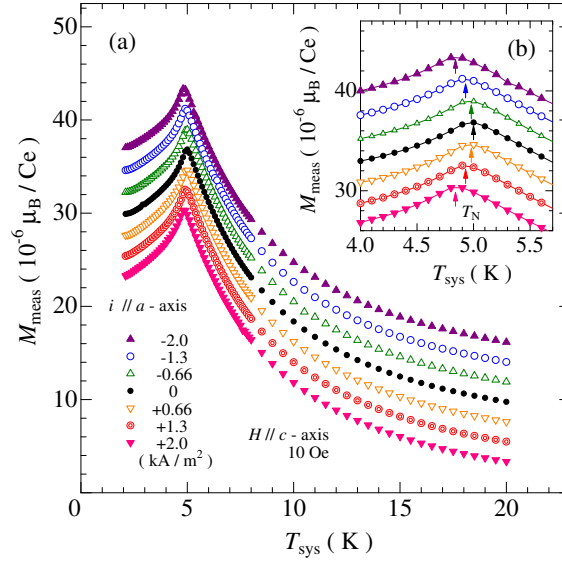


Fig. 2. (Color online) (a) Temperature dependence of magnetization directly obtained from MPMS3 at several i and $H = 10$ Oe. (b) Extended view of the $M_{\text{meas}}-T_{\text{sys}}$ curve around the AFM ordering temperature. The arrows mark each T_N , and the solid lines are guides for the eye.

(Quantum Design MPMS3 or MPMS). To study the ME effect, a constant DC electric current (I) was applied using a source meter (Keithley Inst. Inc. 2401), and the electric current density (i) was estimated from the cross-sectional area of the sample. Two samples were used for this study, where the sizes of samples A and B were approximately $1.8 \text{ mm} \times 7.6 \text{ mm}^2$ and $1.4 \text{ mm} \times 8.2 \text{ mm}^2$, respectively. Two Cu wires with a 0.05 mm diameter were attached to the sample as current leads with a silver paste. The temperature dependences of magnetization were measured from 2 K to 20 K under static magnetic field H and i . Therefore the obtained magnetization data are expressed as $M_{\text{meas}}(H, i, T_{\text{sys}})$, where T_{sys} is the temperature indicated by MPMS3 (or MPMS). A magnetic field was applied by a superconducting magnet and exhibited good stability with some bias owing to the residual magnetic field. We estimated the residual magnetic field to be within ± 4 Oe from the magnetization versus magnetic field curve of Ce_3TiBi_5 .

First, we show the T_{sys} dependence of M_{meas} at $H = 10$ Oe and at several I up to 15 mA ($i = 2.0 \text{ kA/m}^2$) in 5 mA steps in Figs. 2 and determine that the observed M_{meas} includes two extrinsic effects. The black closed circles show the T dependence of magnetization at $i = 0$, which is a usual magnetization ($M_{\chi}(H, T_{\text{sys}})$) induced by H . At 20 K in the paramagnetic region, the magnetization changes from the usual magnetization by applying i . The change expands at the same rate with increasing i . We consider the reason for the change in the paramagnetic region to be an extrinsic effect of induction magnetic field because the

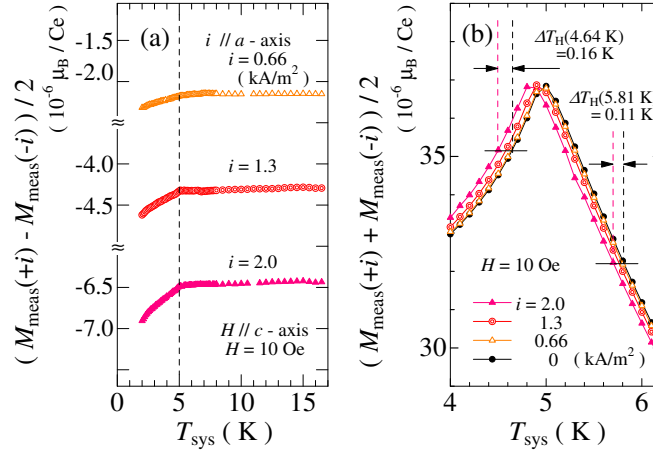


Fig. 3. (Color online) Temperature dependence of the (a) odd and (b) even part of M_{meas} with respect to i at several i . In Fig. 3(a), the broken line indicates a temperature of 5.0 K, and the kink in each curve exists at approximately 5.0 K. The two black solid lines in Fig. 3(b) are horizontal. The curves of the even parts cross the solid line. The difference in temperature between the two crossing point indicates the temperature shift, ΔT_H between $i = 2.0$ kA/m² and $i = 0$ kA/m² are illustrated. The solid lines connecting the symbols are guides for the eye.

Edelstein effect and the ME effect cannot cause it. Current circuit produces some induction magnetic field. A magnetometer will detect the field around the sample as its magnetization. A detailed estimate of the change is performed later by plotting the odd component of M_{meas} with respect to i . Another change in magnetization by applying i in the AFM region exhibits different behavior than that at 20 K, although at first glance it appears to be similar. This is clearly shown when evaluating the difference in magnetization between the positive and negative i . Figure 2(b) shows an enlarged view at approximately T_N . T_N shifted to the lower temperature side by applying i regardless of the positive or negative value of i . However, we confirmed that T_N is independent of the applied current at small current using an experiment on electrical resistivity, in which good thermal contact was achieved between the sample and thermometer. Therefore, the observed T_N shift can be attributed to Joule heating. The DC current to study the ME effect affects the magnitude of the directly obtained magnetization and the temperature of the sample.

To characterize and estimate the change in the paramagnetic region, we show the temperature dependence of $(M_{\text{meas}}(+i) - M_{\text{meas}}(-i))/2$ at several i in Fig. 3(a). Because M_χ induced by H is independent of i , it does not appear on the odd part of M_{meas} . Therefore, we can focus on some current-induced components. The magnitude of the odd part of M_{meas} above T_N increases linearly with an increase in i , and the temperature dependence is very small, where

$(M_{\text{meas}}(+i) - M_{\text{meas}}(-i))/2$ at 15 K and $i = 0.66, 0.13$, and 0.20 kA/m^2 are approximately $-2.15, -4.28$, and $-6.42 \mu_B/\text{Ce}$, respectively. Therefore, M_{meas} contains another part by detecting the induction field (M_c) besides the intrinsic sample's magnetization (M_{sample}): $M_{\text{meas}} = M_{\text{sample}} + M_c$. M_c is independent of T , because the circuit is fixed to the sample-probe and the DC current is constant during the measurement. Thus, M_c depends only on i and is proportional to i . The change of odd part of M_{meas} above T_N is explained well by M_c . We can easily determine M_c from the magnitude of $(M_{\text{meas}}(+i) - M_{\text{meas}}(-i))/2$ above T_N . However, the odd part of M_{meas} below T_N decreases with a decrease in the temperature. This result indicates that the odd part of M_{meas} is made up of two types of current-induced components. The component exhibiting T dependence is considered to be the ME effect owing to the ferroic toroidal state. Next, we estimate the temperature shift owing to the Joule heating. The temperature dependence of $(M_{\text{meas}}(+i) + M_{\text{meas}}(-i))/2$ is shown in Fig. 3(b). Both current-induced components at positive and negative i are canceled out by averaging them in the even part of M_{meas} . Then, only magnetization induced by H remains. Black closed circles correspond to M_χ at $H = 10 \text{ Oe}$ and $i = 0 \text{ kA/m}^2$. These data are not affected by Joule heating. The maximum of the even part of M_{meas} is independent of i , but the temperature exhibiting the maximum value of the even part decreases with increasing i , where the difference in the temperature between $i = 2.0 \text{ kA/m}^2$ and $i = 0 \text{ kA/m}^2$ is approximately 0.15 K . The sample temperature (T) will be ΔT_H higher than T_{sys} because of the Joule heating: $T = T_{\text{sys}} + \Delta T_H$. ΔT_H must be an even function with respect to i because the power of heating (P) generated by the current is proportional to the square of the current: $P \propto i^2$. Consequently, we can estimate ΔT_H at each temperature by obtaining the horizontal difference. The abovementioned results of the odd and even part of M_{meas} confirmed that the abovementioned assumptions for ΔT_H and $M_c(i)$ are valid. The intrinsic sample's magnetization can be extracted from the relation, $M_{\text{sample}}(H, i, T) = M_{\text{meas}}(H, i, T_{\text{sys}} + \Delta T_H) - M_c(i)$, after ΔT_H and M_c are correctly determined.

Figure 4(a) shows $M_{\text{sample}}(T)$ at several i for sample A based on the results in Fig. 2(a). The curve with black closed circles represents $M_{\text{sample}}(T)$ with a zero DC current, namely $M_\chi(T)$ of Ce_3TiBi_5 . Above T_N , $M_{\text{sample}}(T)$ was found to be independent of the DC current and exhibited an identical T dependence. In contrast, $M_{\text{sample}}(T)$ begins to deviate from M_χ just below T_N with a decrease in T . The deviation shows a DC current dependence below T_N . M_{sample} at 3.0 K decreases with increasing i . To confirm the reproducibility of these behaviors, we performed measurements at the same conditions but at $H = 5 \text{ Oe}$ or using another sample of Ce_3TiBi_5 (sample B), as shown in Figs. 4(b) and (c), respectively. The i dependence of the deviation below T_N is clearly observed in $M_{\text{sample}}(T)$ measured at $H = 5 \text{ Oe}$. The magnitude

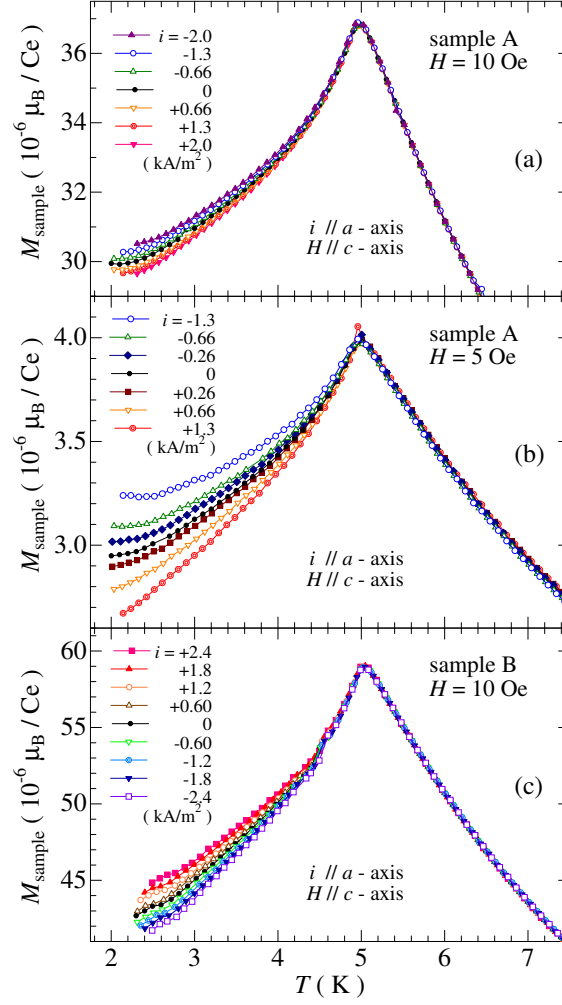


Fig. 4. (Color online) Temperature dependences of intrinsic magnetization M_{sample} at several i for (a) sample A at $H = 10$ Oe, (b) sample A at $H = 5$ Oe, and (c) sample B at $H = 10$ Oe.

of the deviation in Fig. 4(b) is similar to that in Fig. 4(a) at the same applied current and is independent of the magnitude of H . Figure 4(c) shows similar results from a viewpoint of the existence of a deviation only below T_N . However, $M_{\text{sample}}(T)$ increases with an increase in i , which differs from the behavior in sample A. We revealed the existence of the systematically increasing (or decreasing) deviation with an increase in i on $M_{\text{sample}}(T)$ below T_N . This deviation is understood as the component of magnetization owing to the ME effect (M_{ME}). The reason for the difference in the sign of deviation is mentioned in a later paragraph about i dependence of M_{ME} .

We plot $M_{\text{ME}}(T)$ at several i and $H = 10$ Oe in Figs. 5, where $M_{\text{ME}}(T)$ is extracted from $M_{\text{sample}}(T)$ by subtracting $M_{\chi}(T)$. The value of $M_{\text{ME}}(T)$ in Figs. 5(a) and (b) are obtained based on the results in Fig. 4(a) and (c), respectively. Above T_N , M_{ME} is found to be almost

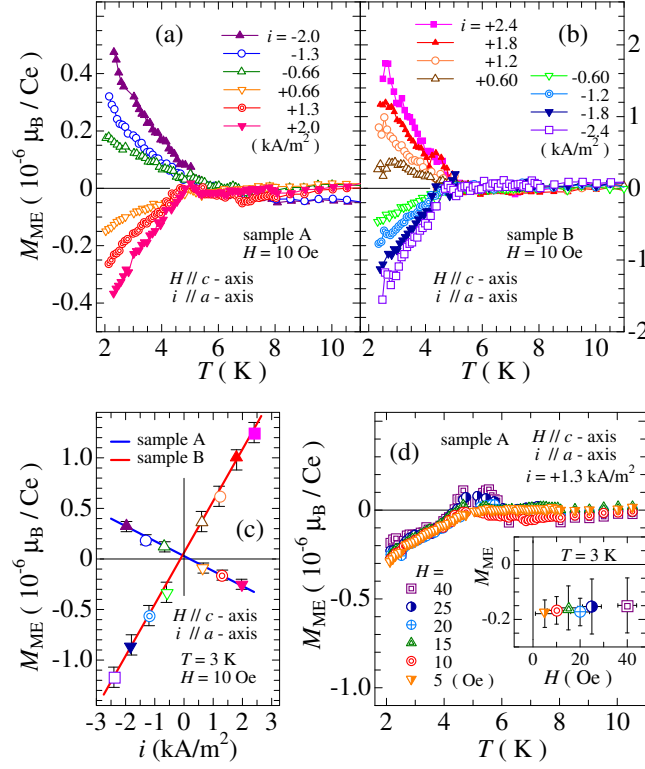


Fig. 5. (Color online) Temperature dependence of the component of the current-induced magnetization, M_{ME} , at several i for (a) sample A and (b) sample B. (c) Electric current dependences of M_{ME} at 3 K for samples A and B. The same symbols indicate the same conditions for H and i . (d) Comparison of the temperature dependence of M_{ME} between different magnetic fields. The inset shows the magnetic field dependence of M_{ME} at 3 K.

independent of temperature and is approximately zero. However, the sudden variation starts to appear just below T_N . The variations in samples A and B exhibit a similar T dependence of M_{ME} . Although it is important to discuss the T dependence of the ME effect, it is not essential to discuss it in detail because our measurements were performed by applying a constant electric current and not a constant field. It is difficult to separately consider the components of the ME effect induced by an electric field and by a current in magnetization, although the observed M_{ME} is essentially caused by the applied electric field in this situation.^{8,9)}

Next, to discuss the i dependence of the magnitude of M_{ME} , we show plots of M_{ME} versus i for samples A and B at $T = 3.0 \text{ K}$ in Fig. 5(c). M_{ME} shows the linear i dependence for both samples A and B, which suggests that M_{ME} linearly increases with an increase in the electric field. Furthermore, M_{ME} for both samples is almost zero at $i = 0$. $\partial M_{ME} / \partial i$ at 3.0 K for samples A and B are $\sim -1.5 \times 10^{-10}$ and $\sim 5.2 \times 10^{-10} \mu_B \cdot \text{m}^2 / (\text{A} \cdot \text{Ce})$, respectively. We consider the sample dependence of the sign and magnitude of $\partial M_{ME} / \partial i$ to be explained by the imbalance of the domain structure of the AFM state. This means that the toroidal moment

of different domains points in the opposite direction and M_{ME} is also induced in the opposite direction. Therefore net M_{ME} , which is a summation over the entire sample, depends on the difference between the total sizes of the two AFM domains. The absolute values of the two values are several times larger than that of UNi_4B of $\sim 9.4 \times 10^{-11}$. However, currently, it is difficult to discuss the magnitude of the ME effect for at least two reasons. The first reason is that the exact electric field applied to the sample is unknown. The second reason is that the observed current-induced magnetization is thought to be not uniform because of the domain structures.

Figure 5(d) shows the T dependence of M_{ME} for sample A at several H . $M_{\text{ME}}(T)$ exhibits an identical curve despite a difference in the magnitude of H , although the measurement accuracy decreases with increase in H . The magnitude of M_{ME} at each magnetic field and $T = 3.0$ K was decided from the T dependence of M_{ME} at several H ($5 \leq H \leq 40$ Oe) and is plotted in the inset in Fig. 5(d). The magnitude of M_{ME} at $T = 3.0$ K is independent of H in this field range, which indicates that M_{ME} at $T = 3.0$ K has a similar value even in a zero magnetic field. The results shown in Figs. 5 suggest that M_{ME} depends only on a DC current and not on a magnetic field.

Finally, we discuss issues related to the AFM ordered state and its domains. Although we consider the sample dependence of M_{ME} to be explained by the imbalance of the domain structure of the AFM state, it remains an unsettled question as to why the net M_{ME} exhibits good reproducibility if the AFM domains are produced randomly. Furthermore, three toroidal moments on three zig-zag Ce chains in a unit cell of Ce_3TiBi_5 will mutually align in a 120-degree orientation, which is parallel to the vertical direction of the plane including a Ce zig-zag chain, as depicted in Fig. 1(b), when Ce_3TiBi_5 has a simple magnetic structure for the AFM ordered state. The net M_{ME} should be zero in this case. Yet, M_{ME} was observed in Ce_3TiBi_5 , and $M_{\text{ME}}(T)$ exhibited good reproducibility in the serial measurements and linearity of the $M_{\text{ME}}-i$ curve. In situations where the detailed magnetic structure was not decided, the origin of net M_{ME} with a finite value was unknown. The following reasons may explain the net M_{ME} : it may reflect a more complex magnetic structure,¹⁸⁾ or defects or impurities may determine how magnetic domains align and lead to good reproducibility. Moreover, in the previous study on UNi_4B ,¹⁶⁾ the discussion acknowledges the partial inconsistency with the theoretical results. Both their and our results may have similar problems because of the ME effect in the metal. Regardless, future work should focus on indicating the magnetic structure of this system. In addition, it is important to reveal the anisotropy of M_{ME} at lower T and the M_{ME} hysteresis behaviors by measuring changes in the magnetic domains.^{7, 19, 20)}

In summary, we carried out magnetization measurements under an applied DC electric current on the metallic compound Ce_3TiBi_5 with Ce zig-zag chains. The current-induced magnetization was observed only below the AFM transition temperature, $T_N = 5.0$ K. This current-induced magnetization exhibits linear dependence with respect to the DC electric current and demonstrates little dependence on the magnetic field, i.e., the behavior persists even in a zero magnetic field. On the basis of these results, we suggest that the current-induced magnetization originated from the ME effect of the ferrotoroidal state on the Ce zig-zag chain structure. However, it is still unclear whether the net M_{ME} is consistent for the bulk behavior. To reveal the ME effect on Ce_3TiBi_5 , future studies that use techniques such as neutron scattering or NMR measurements are needed to determine the magnetic structure with certainty. In addition, magnetization measurements should be conducted at lower temperatures, including measurements of different geometries to study the anisotropy of the ME effect in Ce_3TiBi_5 and that for different measurement procedures to study the effect of magnetic domains.

Acknowledgments

This work was supported by JSPS KAKENHI Grant No. 16K05450, and by Grant Number 18H04322 and JP15H05885 (J-Physics).

References

- 1) I. E. Dzyaloshinskii, Sov. Phys. JETP **10**, 628 (1959).
- 2) D. N. Astrov, Sov. Phys. JETP **11**, 708 (1960).
- 3) V. J. Folen, G. T. Rado, and E. W. Stalder, Phys. Rev. Lett. **6**, 607 (1961).
- 4) T. Kimura, T. Goto, H. Shintani, K. Ishizaka, T. Arima, and Y. Tokura, Nature **426**, 55 (2003).
- 5) J. Wang, J. B. Neaton, H. Zheng, V. Nagarajan, S. B. Ogale, B. Liu, D. Viehland, V. Vaithyanathan, D. G. Schlom, U. V. Waghmare, Science **299**, 1719 (2003).
- 6) N. Hur, S. Park, P. Sharma, J. Ahn, S. Guha, and S. Cheong, Nature **429**, 392 (2004).
- 7) W. Eerenstein, N. D. Mathur, and J. F. Scott, Nature **442**, 759 (2006).
- 8) S. Hayami, H. Kusunose, and Y. Motome, Phys. Rev. B **90**, 024432 (2014).
- 9) H. Watanabe and Y. Yanase, Phys. Rev. B **96**, 064432 (2017).
- 10) M.-T. Suzuki, T. Koretsune, M. Ochi, and R. Arita, Phys. Rev. B **95**, 094406 (2017).
- 11) Y. Yanagi and H. Kusunose, J. Phys. Soc. Jpn. **86**, 083703 (2017).
- 12) S. Hayami, M. Yatsushiro, Y. Yanagi, and H. Kusunose, Phys. Rev. B **98**, 165110 (2018).
- 13) V. M. Edelstein, Solid State Commun. **73**, 233 (1990).
- 14) Y. K. Kato, R. C. Myers, A. C. Gossard, and D. D. Awschalom, Phys. Rev. Lett. **93**, 176601 (2004).
- 15) T. Furukawa, Y. Shimokawa, K. Kobayashi, and T. Itou, Nat. Commun. **8**, 954 (2017).
- 16) H. Saito, K. Uenishi, N. Miura, C. Tabata, H. Hidaka, T. Yanagisawa, and H. Amitsuka, J. Phys. Soc. Jpn. **87**, 033702 (2018).
- 17) G. Motoyama, M. Sezaki, J. Gouchi, K. Miyoshi, S. Nishigori, T. Mutou, K. Fujiwara, Y. Uwatoko, Physica B. **536**, 142-144 (2018).
- 18) T. Katsufuji, JPSJ News and Comments. **15**, 02 (2018).
- 19) H. Schmid, Int. J. Magnetism **4**, 337 (1973).
- 20) T. Arima, D. Higashiyama, Y. Kaneko, J. P. He, T. Goto, S. Miyasaka, T. Kimura, K. Oikawa, T. Kamiyama, R. Kumai, and Y. Tokura, Phys. Rev. B. **70** 064426 (2004).